# Break-Up of $H_2$ in Singly Ionizing Collisions with Fast Protons: Channel-Selective Low-Energy Electron Spectra

C. Dimopoulou[1], R. Moshammer[1], D. Fischer[1], C. Höhr[1], A. Dorn[1], P.D. Fainstein[4],

J. R. Crespo López Urrutia[1], C.D. Schröter[1], H. Kollmus[2],

R. Mann[2], S. Hagmann[2,3], and J. Ullrich[1]

[1]Max-Planck-Institut für Kernphysik, Saupfercheckweg 1, 69117 Heidelberg, Germany

[2]Gesellschaft für Schwerionenforschung, Planckstr. 1, 64291 Darmstadt, Germany

[3]Institut für Kernphysik, August-Euler-Strasse 6, 60486 Frankfurt, Germany

[4]Centro Atómico Bariloche, Comisión Nacional de Energía Atómica, 8400 Bariloche, Argentina

## Abstract

Dissociative as well as non-dissociative single ionization of $H_2$ by 6 MeV proton impact has been studied in a kinematically complete experiment by measuring the momentum vectors of the electron and the $H^+$ fragment or the $H_2^+$ target ion, respectively. For the two ionization pathways, the coincident electron spectra reveal significantly different structures which are due to autoionization of the singly or doubly excited states of $H_2$, effects beyond the Born-Oppenheimer approximation that explicitly involve the coupling between the electronic and the nuclear motion of the molecule.

1

Single ionization of atoms by fast ion impact has been studied extensively experimentally as well as theoretically for many years [1, 2] mainly by investigating doubly differential electron emission spectra. Fully differential cross sections, as available for electron impact ionization since 1969 [3] (for a review see [4]), have not become accessible experimentally before 2000 with a lot of surprising results [5, 6] (for a review see [7]). As far as molecular targets are concerned, $H_2$ has been the prototype system because it is the simplest diatomic molecule (see e.g. [1, 8, 9, 10, 11]) and, therefore, has attracted considerable attention recently [12]. The molecular nature of the target introduces several new challenging aspects to the collision problem due to the (non-Coulombic) shape of the target potential, the coupling between electronic and nuclear motion giving rise to additional reaction channels (dissociative ionization), and the two-center geometry of the target leading to interference effects in analogy to Young's double slit experiment [12, 13]. Besides these fundamental aspects, charged particle induced ionization of molecules plays a central role in many applications like e.g. cancer therapy with fast ions. There, in particular the production of low-energy electrons is of relevance because they effectively destroy large molecules in biological tissue [14] .

In single ionization of $H_2$ two possible pathways leading to different reaction products can be distinguished (fig. 1). First, in what we call pure ionization, a stable, possibly vibrationally excited $H_2^+$ ion remains after the removal of one electron during the collision, as illustrated by channels 1a and 1b. Second, with a small probability of a few percent of all ionization events [10, 17], the molecule dissociates into an $H^+$ and an H atom (dissociative ionization). The latter happens either by the creation of an excited molecular ion which dissociates since all $(H_2^+)^*$ states are repulsive in the Franck-Condon region or by populating the vibrational continuum of the ground state of $H_2^+$, resulting into dissociation into an $H^+$ and an $H(1s)$ (ground state dissociation).

Most detailed information about the contribution of all channels and the dynamics involved can be obtained in a kinematically complete experiment. For dissociative ionization for instance, ionization plus excitation (channel 2a in fig. 1) can be separated from ground-state dissociation (channels 2b and 2c) using the fact that the kinetic energy of the $H^+$ from the former is typically of the order of a few eV, whereas from the latter it is in the sub-eV range [18]. Until now the experiments focused either on electron emission characteristics [8, 9, 12] or on the measurement of the nuclear fragments only [10, 11].

In this Letter we report on the first coincident detection of the electron and the charged nuclear fragments resulting from single ionization of $H_2$ by proton impact (projectile velocity: $v_p = 15.5$ a.u., perturbation: $Z_P/v_p = 0.06$ in a.u. where $Z_p$ is the projectile charge). Using a "Reaction Microscope" [19] we have recorded the electron energy spectra resolved down to 0.1 eV for both dissociative and pure ionization. For the latter the measurement represents a kinematically complete experiment, whereas this is not the case for dissociative ionization since the H atom has not been detected. It has been frequently argued (see [12] and references therein) that, as far as single ionization is concerned, the cross section of $H_2$ is equal to that of two H atoms times an oscillatory term representing the interference caused by the coherent electron emission from the two centers. The comparison of our data with predictions of a state-of-the-art CDW-EIS calculation (continuum-distorted-wave eikonal-initial-state) [20] taking such interference effects into account provides convincing evidence that this is not true, at least not for low-energy electron emission. Distinct differences appear that can be explained only by taking into account the molecular nature of the target. Here, particular attention will be given to the role of autoionization of singly and doubly excited states of $H_2$, effects that involve not only the electronic but also the nuclear motion of the molecule.

3

The experiment was performed at the Max-Planck-Institute in Heidelberg using a multi-electron recoil-ion momentum spectrometer ("Reaction Microscope" [21]). A well-collimated (1 mm × 1 mm), pulsed (pulse length ≈ 1ns, repetition rate = 289 kHz) proton beam (beam current = 0.5 nA) with an energy of 6 MeV from the Tandem accelerator crosses in the Reaction Microscope a beam of $H_2$ molecules provided by a supersonic gas jet. As a result of the supersonic expansion the target molecules cool to a temperature of less than 10 K and relax into their vibrational ground state. The emitted electrons and the recoil ion were extracted into opposite directions along the projectile beam axis (longitudinal direction) by a weak (4.5 V/cm) electric field over 11 cm and were detected by two-dimensional position sensitive detectors. A longitudinal uniform magnetic field of 14 G confined the transverse motion of the electrons, such that all electrons with $E_e < 35$ eV were detected with the full solid angle. The mass of the recoil ion ($H_2^+$ or $H^+$) and the complete momentum vectors of both, recoil ion and electron, are determined from their measured absolute times-of-flight and positions on the detectors. The $H_2^+$ ions were detected for transverse momenta $p_\perp \leq 2.9$ a.u., covering essentially the full solid angle for pure ionization. For the $H^+$ ion, the maximum transverse momentum acceptance was $p_\perp \leq 2.3$ a.u., corresponding to energies of less than 40 meV for $p_{\parallel} = 0$, covering a solid angle of approximately 10 % for ground state dissociation. The achieved momentum resolution for the $H_2^+$ recoil ions was $\Delta p_{r\parallel} = 0.1$ a.u. in the longitudinal and $\Delta p_{r\perp} = 0.3$ a.u. in the transverse directions, respectively. For the electrons we estimated $\Delta p_{e\parallel} \cong 0.05$ a.u. and $\Delta p_{e\perp} = 0.1$ a.u.. The transverse momentum transfer of the projectile is calculated event by event from the transverse momenta of the electron and the recoiling $H_2^+$ ion $\mathbf{q}_\perp = ( \mathbf{p_{e\perp}} + \mathbf{p_{r\perp}} )$. The resolution in the determination of $q_\perp$ is estimated to be $\Delta q_\perp \cong 0.3$ a.u.. The total momentum transfer is given by $\mathbf{q} = \mathbf{q}_\perp + q_{min} \cdot \hat{u}_p$ , where $\hat{u}_p$ is the unit vector along the initial projectile velocity with $\hat{u}_p \cdot \mathbf{q}_\perp = 0$. The small quantity $q_{min} = (I$

+ $E_e$)/$v_p$ < 0.1 a.u. (for $v_p$ = 15.5 a.u. and $E_e$ < 35 eV) is the minimum momentum transfer (corresponding to zero degree scattering) required to overcome the binding energy I = 15.4 eV and to promote the electron into a continuum state with energy $E_e$.

The electron energy distributions integrated over all emission angles for pure and dissociative ionization as well as the theoretical cross sections calculated within the CDW-EIS are shown in fig. 2(a). In the theoretical model the initial state of $H_2$ is approximated by a superposition of two hydrogenic orbitals centered at each nucleus with a separation given by the equilibrium internuclear distance (R = 1.4 a.u.) and an effective charge of $Z_{eff}$ = 1.19 to correctly reproduce the electronic binding energy. The resulting cross section for emission of an electron with momentum vector $\mathbf{k_e}$ is equal to the one for ionization of two independent effective H atoms multiplied by $\left[ 1 + \dfrac{\sin(|\mathbf{k_e} - \mathbf{q}| R)}{|\mathbf{k_e} - \mathbf{q}| R} \right]$, which represents the interference caused by the two H centers for random orientation of the molecular axis (for details see [20]). Molecular effects beyond this, are not considered in this model. The CDW-EIS calculation predicts a total cross section for $E_e \leq$ 35 eV of $\sigma_{H_2^+}$ = 7.35 × $10^{-18}$ cm$^2$. The experimental cross section $d\sigma_{H_2^+} / dE_e$ for pure ionization has been normalized to the theoretical one in the region 2 eV $\leq E_e \leq$ 35 eV. For dissociative ionization $d\sigma_{H^+} / dE_e$ has been normalized to the known contribution of ground state dissociation, which is 1.4 % of $\sigma_{H_2^+}$ [10, 17], assuming the electron emission to be independent on the energy and angular distribution of the H$^+$, as follows from our data.

Two main features appear in the electron spectra. First, the data from pure ionization are in reasonable overall agreement with the CDW-EIS calculation except for very low electron energies $E_e$ < 1 eV where a significant enhancement of the cross section is observed. Second, at $E_e$ around

5

12 eV a distinct difference appears in the slope of the cross sections between pure and dissociative ionization. In order to enhance the visibility of these structures, the experimental data for both pathways have been divided by the CDW-EIS calculation. These ratios are shown in fig. 2(b). In what follows, the two features above will be discussed separately.

The enhancement of the cross section for pure ionization (pathway 1) in the sub-eV region is due to the presence of autoionizing channels indicating a breakdown of the Born-Oppenheimer approximation. From high-resolution studies [22, 23] and systematic theoretical work [24, 25, 26], it is well established that photoionization of $H_2$ just below and within the first eV above threshold (more precisely from 15.3 to 16.6 eV) is dominated by autoionization from rovibrational levels of singly excited bound Rydberg states of $H_2$. They correspond to an $H_2^+$ ground state plus one electron excited to a Rydberg state with quantum number $n$. As depicted in fig. 1 (channel 1b), their potential curves lie within a few eV below the ground state of $H_2^+$ and are essentially parallel to it, particularly for those with $n \geq 4$. Higher vibrational levels of these states have energies above the ionization potential of $H_2$ and therefore autoionize by converting energy from the vibrational motion into kinetic energy of the outgoing electron: The electron can be viewed to autoionize by scattering on the ion core.

This vibrational autoionization (channel 1b) is substantially different from the direct ionization to the continuum (channel 1a) and one expects differences to become evident in highly differential cross sections at $E_e$ above and below about 2 eV. In fig. 3 (upper row) we present the fully differential cross section (FDCS) $d^5\sigma/d\mathbf{q}_\perp d\mathbf{k_e}$ for electrons emitted into the scattering plane, i.e. the plane defined by the momentum vectors of the incoming and the scattered projectile, as a function of the polar electron emission angle relative to the initial projectile direction, for a fixed electron energy $E_e = 2.6$ eV and two different magnitudes of the momentum transfer q. As

6

expected for the direct ionization (channel 1a) the agreement between the data and the CDW-EIS on an absolute scale is reasonably good. The large peak (the so-called binary peak [3]) in the direction of the momentum transfer **q** (practically at 90°) corresponds to electrons ejected by a binary interaction with the projectile, whereas the smaller peak in the direction of **–q** (the so-called recoil peak) corresponds to the case when most of the momentum transfer is taken by the recoil ion. With increasing q the recoil peak systematically decreases in magnitude relative to the binary peak.

At very low electron energies ($E_e$ = 0.2 eV) the comparison of the FDCS with theory reveals distinct discrepancies (lower row in fig. 3), not only in the magnitude of the cross sections, which would have been already expected from fig. 2, but more severely, in the absolute value and the q-dependence of the ratio between the recoil and the binary peak. In sharp contradiction to the theoretical prediction, this ratio is approximately close to one and does not change with increasing q, a feature that can be well understood for vibrational autoionization (channel 1b): Making use of the analogy between charged particle impact excitation (ionization) and photoionization for small momentum transfers and electron energies [27], we expect that the angular distribution of the autoionized electrons is essentially a dipolar one with respect to the momentum transfer axis. In fact, the autoionization can be described as a dipole-like photoexcitation of the molecule to a bound intermediate electronic state followed by a transition of the electron into a continuum *p*-state after transfer of energy from the vibrating nuclei to the electron, leaving the $H_2^+$ ion in its $1s\sigma_g$ ground state.

Returning to the discussion of dissociative ionization (pathway 2), a broad maximum appears in comparison with the CDW-EIS prediction at electron energies around 12 eV up to 35 eV, as shown in fig. 2(b). This feature can be explained by the contribution of an additional

7

channel, namely the excitation of a doubly excited Rydberg state of $H_2$ autoionizing by an electronic transition into the vibrational continuum of the ground state of $H_2^+$, as depicted by channel 2c in fig. 1(see also [28]). After an initial excitation to the doubly excited state the atoms begin to separate along the repulsive potential curve and, thus, gain kinetic energy $\Delta E$. At some internuclear distance the molecule autoionizes into a particular vibrational level of $H_2^+$. If $\Delta E$ is sufficiently large the molecule dissociates into an $H^+$ and an $H(1s)$. Both, electron and photon impact studies [17, 29, 30] have revealed the importance of doubly excited states in dissociative ionization where the ratio of the yield of $H^+$ with respect to $H_2^+$ ions has been measured as a function of the energy transferred to the molecule. Although the first excited state ($2p\sigma_u$) of $H_2^+$ is not accessible in the Franck-Condon region at energies below 28 eV, a broad maximum appears around 30 eV. For very low-energy $H^+$, as it is the case in our experiment, an additional small structure appears at around 25 eV. Calculations [31, 32] have attributed the maximum at 30 eV to channel 2c and the structure at lower energies to its interference with channel 2b (fig. 1). Given that 18.1 eV is the threshold for ground state dissociation, the above structures correspond to the observed enhancement at $E_e$ around 12 eV.

In summary, the electron energy spectra for pure ionization of $H_2$ and that coincident with dissociation have been measured for the first time. The comparison with the CDW-EIS predictions allowed the identification of sizeable contributions from purely molecule-specific electron emission channels. Surprisingly, significant differences are observed even though the kinetic energy released in the dissociation amounts to only a few tens of meV. Within the same frame, FDCSs have been obtained for pure ionization, which, to our knowledge, have not been accessible so far for ion impact on $H_2$. The observed differences are due to the autoionization of (singly or

8

doubly) excited states of $H_2$, which decay through the coupling between the nuclear and the electronic motion in the molecule.

**Figure captions**

**Fig. 1:** Schematic potential curves for $H_2$ and $H_2^+$ illustrating the different single ionization pathways (for detailed molecular potential curves see [15, 16]).

**Fig. 2** (a): Electron energy distributions for single ionization of $H_2$ by 6 MeV proton impact. Triangles: experimental data for pure ionization. Circles: experimental data for dissociative ionization. Solid lines: CDW-EIS results. (b): Ratios of experimental to theoretical cross sections.

**Fig. 3:** FDCS for electrons emitted into the scattering plane for pure ionization of $H_2$ by 6 MeV proton impact. Upper row: The electron energy $E_e = 2.6$ eV is fixed and the values of the momentum transfer are q = 0.5 and 0.8 a.u., respectively. Lower row: $E_e = 0.2$ eV, same momentum transfer values. Solid lines: CDW-EIS results. The cross sections are given in $10^{-18}$ $cm^2/au^2$.

**References**

[1]    M.E. Rudd, Y.-K. Kim, D.H. Madison, and T.J. Gay, Rev. Mod. Phys. **64**, 441 (1992)

[2]    N. Stolterfoht, R.D. DuBois, and R.D. Rivarola, *Electron Emission in Heavy Ion-Atom Collision*s, Springer Series on Atoms and Plasmas (1997)

[3]    H. Ehrhardt, M. Schulz, T. Tekaat, and K. Willmann, Phys. Rev. Lett. **22**, 89 (1969)

[4]    A. Lahmam-Bennani, J. Phys. B **24**, 2401 (1991)

[5]    M. Schulz, R. Moshammer, D. Fischer, H. Kollmus, D.H. Madison, S. Jones, and J. Ullrich, Nature (London) **422**, 48 (2003)

[6]    D.H. Madison, D. Fischer, M. Foster, M. Schulz, R. Moshammer, S. Jones, and J. Ullrich, Phys. Rev. Lett. **91**, 253201 (2003)

[7]    J. Ullrich and S. Shevelko,  *Many Particle Quantum Dynamics in Atomic Fragmentation*, Springer Series on Atoms and Plasmas (2003)

[8]    L.H. Toburen and W.E. Wilson, Phys. Rev. A **5**, 247 (1972)

[9]    A.K. Edwards *et al.,* Phys. Rev. A **37**, 3697 (1988);  Phys. Rev. A **42,** 1367 (1990)

[10]    I. Ben-Izthak, Vidhya Krishnamurthi, K. D. Carnes, H. Aliabadi, H. Knudsen, U. Mikkelsen, and B. D. Esry, J. Phys. B **29**, L21-L28 (1996)

[11]    R. M. Wood, A. K. Edwards, and M. F. Steuer, Phys. Rev. A **15**, 1433 (1977)

[12]    N. Stolterfoht *et al.,* Phys. Rev. Lett. **87**, 023201 (2001)

[13]    H.D. Cohen and U. Fano, Phys. Rev. **150**, 30 (1966)

[14]    B. Boudaiffa, P. Cloutier, D. Hunting, M.A. Huels, and L. Sanche,

        Science **287**, 1658 (2000)

[15]    T.E. Sharp, At. Data **2**, 119 (1971)

[16]    S.L. Guberman,  J. Chem. Phys. **78**, 1404 (1983)

[17]    C. Backx, G.R.Wight, and M.J. Van der Wiel, J. Phys. B **9**, 315 (1976)

[18]    W. Wolff, I. Ben-Izthak, H.E. Wolf, C.L. Cocke, M.A. Abdallah, and M. Stöckli,

        Phys. Rev. A **65**, 042710 (2002)

[19]    J. Ullrich, R. Moshammer, A. Dorn, R. Dörner, L.Ph. H. Schmidt, and

         H. Schmidt-Böcking, Rep. Prog. Phys. **66**, 1463 (2003)

[20]    M.E. Galassi, R.D. Rivarola, P.D. Fainstein, and N. Stolterfoht,

        Phys. Rev. A **66**, 052705 (2002)

[21]    R. Moshammer, M. Unverzagt, W. Schmitt, J. Ullrich, and H. Schmidt-Böcking,

        Nucl. Instrum. Methods Phys. Res., Sect. B **108**, 425 (1996)

[22]    W.A. Chupka and J. Berkowitz, J. Chem. Phys. **51**, 4244 (1969)

[23]    P.M. Dehmer and W.A. Chupka, J. Chem. Phys. **65**, 2243 (1976)

[24]    R.S. Berry and S.E. Nielsen, Phys. Rev. A **1**, 383 and 395 (1970)

[25]    G. Herzberg and Ch. Jungen, J. Mol. Spectrosc. **41**, 425 (1972)

[26]    U. Fano, Phys. Rev. A **2**, 353 (1970)

[27]   M. Inokuti, Rev. Mod. Phys. **43**, 297 (1971)

[28]   K. Kirby, T. Uzer, A.C. Allison, and A. Dalgarno,  J. Chem. Phys. **75**, 2820 (1981)

[29]   Y.M. Chung, E.-M. Lee, T. Masuoka, and J.A.R. Samson, J. Chem. Phys. **99**, 885 (1993)

[30]   Z.X. He, J.N. Cutler, S.H. Southworth, L.R. Hughey and J.A.R. Samson,

       J. Chem. Phys. **103**, 3912 (1995)

[31]   I. Sánchez and F. Martín, Phys. Rev. Lett. **79**, 1654 (1997)

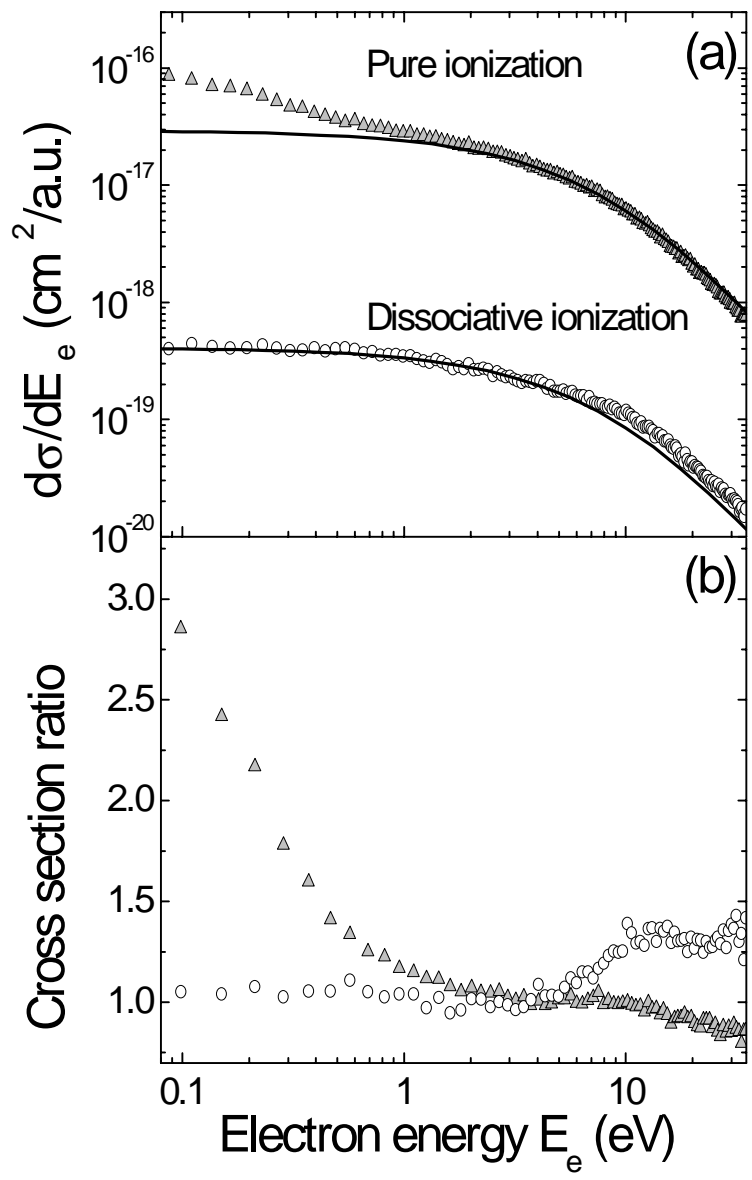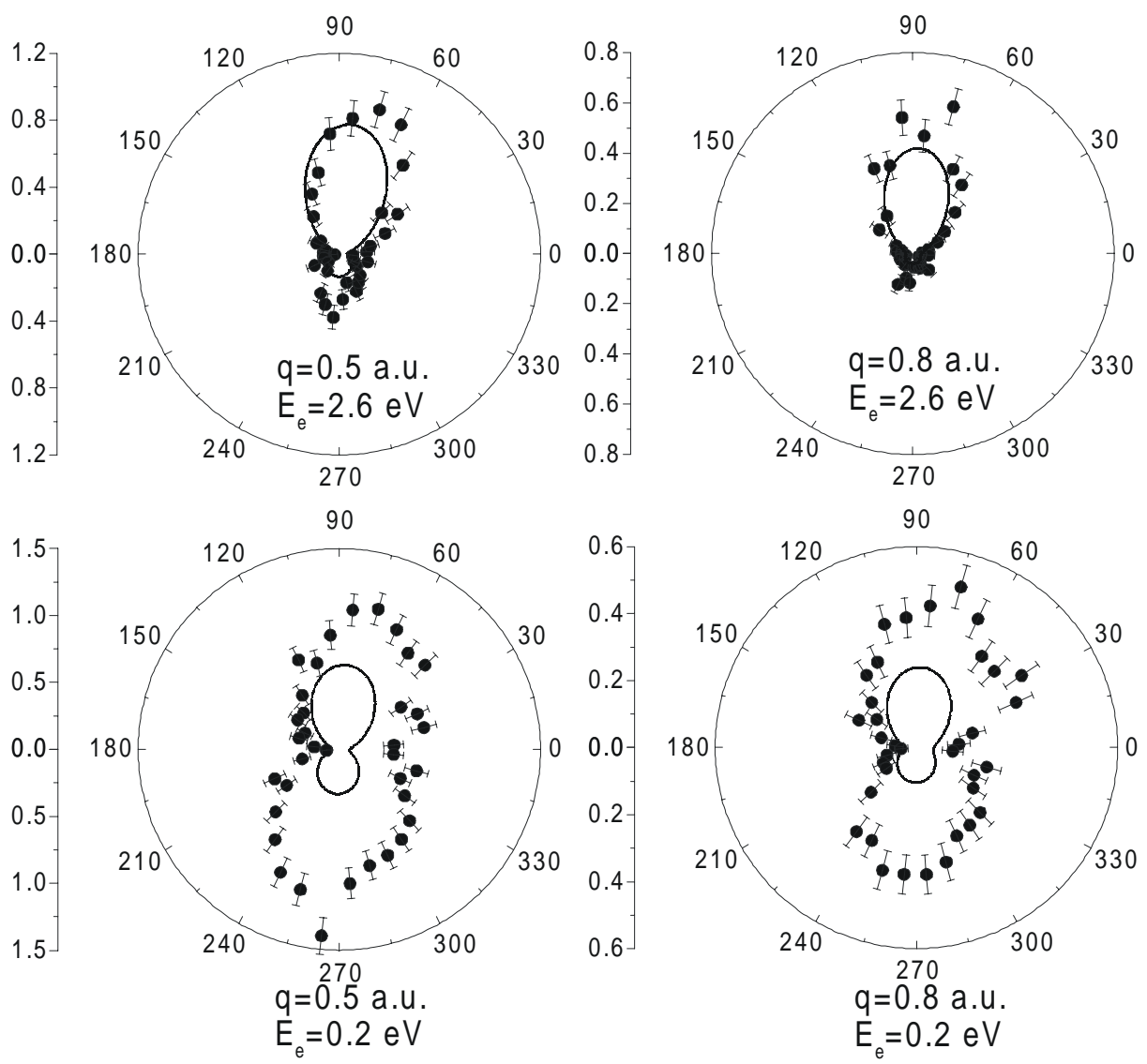[32]   I. Sánchez and F. Martín, J. Chem. Phys. **107**, 8391 (1997)
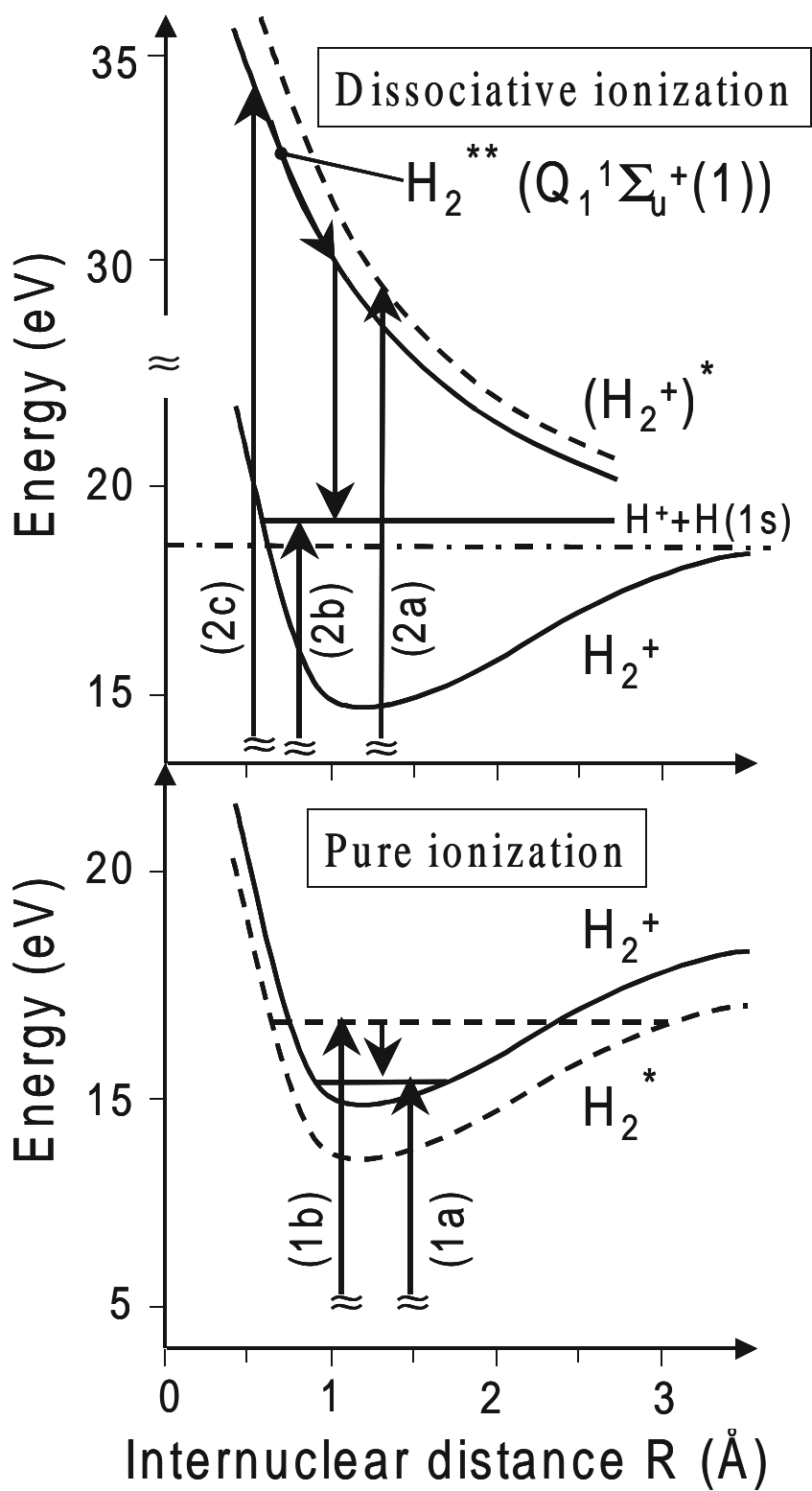
Figure 1

Figure 2

Figure 3